Oecologia (2022) 200:51–64
https://doi.org/10.1007/s00442-022-05250-4

PHYSIOLOGICAL ECOLOGY – ORIGINAL RESEARCH

Safety–efficiency tradeoffs? Correlations of photosynthesis, leaf hydraulics, and dehydration tolerance across species

Dongliang Xiong[1] · **Jaume Flexas**[2]

Received: 21 January 2022 / Accepted: 23 August 2022 / Published online: 30 August 2022

Abstract

The tradeoffs between carbon assimilation and hydraulic efficiencies and drought-tolerance traits on different scales are considered a central tenet in plant ecophysiology; however, no clear tradeoff between these traits has emerged in previous studies using woody angiosperms or grasses by investigating several hydraulic tolerance and gas exchange efficiency and/or water transport efficiency traits. In this study, we measured numerous efficiency, resistance, and leaf anatomical traits, including light-saturated gas exchange, leaf hydraulic vulnerability curves, pressure–volume curves, and leaf anatomical traits, in seven species with diverse drought tolerance. A substantial variation in photosynthetic rate, stomatal conductance, mesophyll conductance, maximum leaf hydraulic conductance (K_{max}), mesophyll anatomical traits, and leaf vein density across species was observed. Both mesophyll conductance and K_{max} were related to leaf anatomical traits, but other gas exchange traits were decoupled from K_{max}. Although the efficiency and tolerance traits varied widely across estimated species, no clear trade-off between safety traits and efficiency traits was observed. These findings suggested that postulated leaf-level drought tolerance-carbon assimilation and hydraulic efficiency tradeoff does not exist among distant species and that the fact that different leaf anatomical traits determine efficiency and tolerance capacity might contribute to the lack of such tradeoffs.

Keywords Photosynthesis · Hydraulic · Drought avoidance · Drought tolerance · Trade-offs · Leaf anatomy

Introduction

One central theme in plant ecology is the trade-offs between the efficiency of water transport and the resistance of the vascular system to embolisms and, at the leaf scale, the mechanism of the trade-off between efficiency and tolerance is widely reflected in the so-called leaf economics spectrum (Wright et al. 2004; Onoda et al. 2017; Xiong and Flexas 2018). Within the efficiency-tolerance context, fast-growing species generally combine low structural investment with high assimilation and low-stress tolerance; in contrast, the slow-growing species associated with high structure investment, low assimilation rate, and stress-tolerant leaves (Wright et al. 2004). Besides this, over the past decades, many studies have investigated another aspect of the general trade-off, i.e. the trade-offs between the efficiency of water transport and the tolerance of the vascular system from embolisms in both stem and leaf (Blackman et al. 2010; Nardini et al. 2012; Ocheltree et al. 2016). In these studies, the tolerance of the vascular system to embolism was generally quantified in terms of P_x, that is the water potential values inducing x% loss of hydraulic conductance (a list of traits, symbols, and units, see Table 1).

The efficiency-tolerance tradeoff hypothesis in woody stems was supported by some studies, but not others (reviewed by Gleason et al. 2016). Although there are a few studies that investigated the trade-off between efficiency

Communicated by Kouki Hikosaka.

✉ Dongliang Xiong
dlxiong@mail.hzau.edu.cn

Jaume Flexas
jaume.flexas@uib.es

[1] National Key Laboratory of Crop Genetic Improvement, Hubei Hongshan Laboratory, MOA Key Laboratory of Crop Ecophysiology and Farming System in the Middle Reaches of the Yangtze River, College of Plant Science and Technology, Huazhong Agricultural University, Wuhan 430070, Hubei, China

[2] Research Group on Plant Biology Under Mediterranean Conditions, Instituto de Investigaciones Agroambientales y de Economía del Agua (INAGEA), Universitat de Les Illes Balears, Carretera de Valldemossa Km 7.5Illes Balears, 07121 Palma, Spain

Table 1 List of leaf traits symbols and units

	Symbol	Trait	Unit
Efficiency	A	Light-saturated photosynthetic rate	μmol m^{-2} s^{-1}
	g_s	Stomatal conductance to CO_2	mol m^{-2} s^{-1}
	g_m	Mesophyll conductance to CO_2	mol m^{-2} s^{-1}
	g_t	Total conductance to CO_2	mol m^{-2} s^{-1}
	g_mE	Mesophyll conductance fitted from A/C_i curve	mol m^{-2} s^{-1}
	K_{leaf}	Leaf hydraulic conductance	mmol m^{-2} s^{-1} MPa^{-1}
	K_{max}	Maximum K_{leaf}	mmol m^{-2} s^{-1} MPa^{-1}
	V_{cmax}	Maximum carboxylation efficiency	μmol m^{-2} s^{-1}
	J_{max}	Maximum rate of electron transport	μmol m^{-2} s^{-1}
Tolerance	P_{50}	Leaf water potential at 50% decline of K_{leaf}	MPa
	P_{80}	Leaf water potential at 80% decline of K_{leaf}	MPa
	π_0	Osmotic potential at full turgor	MPa
	π_{tlp}	Turgor loss point	MPa
	ε	Modulus of elasticity	MPa
Anatomy	LMA	Leaf mass per leaf area	g m^{-2}
	FEV	Free ending vein number per leaf area	mm^{-2}
	VLA	Leaf vein length per leaf area	mm mm^{-2}
	VLA_{major}	Major vein length per leaf area	mm mm^{-2}
	VLA_{monor}	Minor vein length per leaf area	mm mm^{-2}
	T_{leaf}	Leaf thickness	mm
	LD	Leaf density	mg mm^{-3}
	f_{IAS}	Fraction of leaf mesophyll volume occupied by intercellular air space	%
	T_{upE}	Up epidermis thickness	μm
	$T_{palisade}$	Palisade thickness	μm
	T_{spongy}	Spongy thickness	μm
	T_{lowE}	Low epidermis thickness	μm
	T_{cw}	Cell wall thickness	μm
	S_m	Total mesophyll cell surface area exposed to intercellular air space per unit of leaf surface area	m^{-2} m^{-2}
	S_c	Total chloroplasts surface area exposed to intercellular air space per unit of leaf surface area	m^{-2} m^{-2}
Others	ψ_{inital}	Initial leaf water potential	MPa
	Ψ_{final}	Final leaf water potential	MPa
	E	Water flux rate per leaf area	mmol m^{-2} s^{-1}

and tolerance at the leaf scale, these studies also produced mixed results (Blackman et al. 2010; Nardini et al. 2012; Ocheltree et al. 2016). For instance, Blackman et al. (2010) investigated maximum leaf hydraulic conductance (K_{max}) and P_{50} of 20 woody angiosperm species and found no significant correlation between K_{max} and P_{50}. In contrast, a significant tradeoff between K_{max} and P_{50} was observed across six woody species (Nardini et al. 2012) as well as across nine grass species (Ocheltree et al. 2016). The reason for these discrepancies is unclear, although a recent study suggested that the efficiency-tolerance traits tradeoff is influenced by seasonal drought (Liu et al. 2021).

Due to the important role of water transport capacity within the soil–plant-atmosphere continuum in determining CO_2 diffusion conductance from leaf surface to chloroplast (Brodribb et al. 2007; Xiong et al. 2017), the light-saturated photosynthetic rate (A), a key determinant of growth capacity, is assumed to be represented by K_{max}. This means that if an efficiency-tolerance tradeoff exists in the water transport system of plants, it should translate to a trade-off between hydraulic safety and A. However, a recent study showed that the correlation between K_{max} and A does not exist across nine grass species, which indicated that hydraulic efficiency may decouple from carbon gain efficiency (Ocheltree et al. 2016). Indeed, the hydraulic resistance within leaves represents only a part of the hydraulic resistance of the soil–plant–atmosphere continuum (Sack et al. 2003; Sack and Holbrook 2006). Therefore, even if an efficiency

vs tolerance trade-off in the hydraulic pathway exists at the organ level, it may not necessarily translate into a trade-off in carbon assimilation efficiency vs drought tolerance.

Beyond hydraulic vulnerability parameters, the leaf water potential at turgor loss point (π_{tlp}), i.e. the leaf water potential (ψ_{leaf}) at which the leaf cell turgor pressure is zero, was suggested to be strongly related to ecological drought tolerance and species distributions relative to water supply within and across biomes (Tyree and Jarvis 1982; Bartlett et al. 2012). Practically, the $\pi_{tlp,}$ together with other parameters, including the bulk modulus of elasticity (Ɛ) and osmotic potential at full hydration (π_0), are typically calculated from a plot of ψ_{leaf} against water volume in drying leaves, known as the pressure–volume (PV) curve. Previous studies have suggested that plants with low π_{tlp} tend to maintain high stomatal conductance, hydraulic conductance, photosynthetic gas exchange, and growth under low soil water availability conditions (Farrell et al. 2017; Trueba et al. 2019; Sorek et al. 2021). Importantly, while P_x reflects the tolerance water transport system of entire leaves, PV curve parameters mainly reflect the ability of mesophyll tissues, where the carbon assimilation occurs, to tolerate drought (Tyree and Jarvis 1982; Bartlett et al. 2012). Therefore, if the trade-off in carbon assimilation efficiency vs drought tolerance exists, the gas exchange should tightly correlate with PV curve parameters. Yet, the trade-off in carbon assimilation efficiency vs cellular drought tolerance has not been integrated and directly compared experimentally.

According to the leaf economics spectrum theory, both efficiency and tolerance are related to the investment in leaf structural components. On the one hand, numerous studies have investigated the influences of anatomical traits on K_{leaf} and photosynthetic traits across species and/or environmental conditions (Niinemets et al. 2002; Buckley et al. 2015; Buckley 2015; Caringella et al. 2015; Tosens et al. 2016; Xiong et al. 2017). It has been suggested that K_{max} is related to vein traits, including vein length per leaf area (VLA), free vein endings (FVEs), and xylem conduit numbers and diameters in both major and minor veins. In addition to leaf veins, it is now recognized that the K_{max} is also highly related to the mesophyll anatomy (Rockwell et al. 2014; Buckley et al. 2015, 2017; Buckley 2015; Xiong et al. 2017), and in fact, a leaf anatomical based outside-xylem water flow model, MOFLO, has been developed by Buckley et al. (2015). On the other hand, the influences of vein traits and mesophyll anatomical traits on drought tolerance were also suggested in many studies (Blackman et al. 2010; Scoffoni et al. 2011, 2016a, 2017; Blonder et al. 2012; Binks et al. 2016). For instance, Scoffoni et al. (2016a) showed that drought-induced decline in hydraulic conductance inside leaf veins was tightly correlated with conduit numbers in the midrib but independent of conduit number and size in minor veins. Mesophyll anatomical traits change dramatically due to the dehydration introduced leaf shrinkage and thus contributed to K_{ox} vulnerability (Blonder et al. 2012; Scoffoni et al. 2014, 2017). However, the role of the leaf anatomy in the tradeoff between efficiency and safety remains unclear.

In this study, we investigated the hydraulic efficiency and tolerance traits, gas exchange, PV traits, and leaf anatomy traits in seven species phylogenetically distant, also varying in leaf habit and drought tolerance. The aim of this study was to assess the following: (1) whether the carbon assimilation efficiency vs drought tolerance trade-off at the leaf level exists across species; and (2) what are the most general physiological and structural bases of carbon assimilation and hydraulic efficiencies and dehydration tolerance traits on leaf level.

Materials and methods

To test the tradeoffs of carbon assimilation and hydraulic efficiencies and drought tolerance/avoidance traits across different species, seven species of diverse phylogeny, origin, life form, and, particularly, their drought tolerance based on literature investigation (details see Table 2), growing in a common garden at the campus of the University of Illes Balears, Palma de Mallorca (Illes Balears, Spain) were used for the study. The species *Nerium oleander* L., *Platanus occidentalis* L., and *Glycine max.* L. were measured in July 2015, and the species of *Populus nigra* L., *Ceratonia siliqua* L., *Ginkgo biloba* L., and *Gossypium hirsutum* L. were measured in July 2016. In the current study, measurements were conducted to 50–60-day old *G. max* and 70–80-day old *G. hirsutum* plants. For other species, mature plants were randomly selected. There were no extreme climatic events during and before the measurements conducted and meteorological data of the site can be found at http://plantmed.uib.es/Ingles/INTRANET.html.

Gas exchange

An open-flow gas exchange system (LI-6400XT, LI-COR, Lincoln, NE, USA) with an integrated fluorescence leaf chamber (LI-6400-40, LI-COR) was used to measure leaf gas exchange and chlorophyll fluorescence simultaneously. The sun exposed leaves on the east side of canopies were selected for each species, and the CO_2 response curves were measured in three to six individuals in situ. The day before the gas exchange measurement conducted, the plants were fully irrigated. The gas exchange measurement to trees was a little challenged, and a stepladder was used to raise the gas exchange system if necessary. The light intensity, block temperature, and flow rate inside the chamber were set to 1500 μmol m^{-2} s^{-1} (10% blue light), 25 ℃, and 300 μmol s^{-1}, respectively. The average vapor pressure

Table 2 The variation of leaf mass per area (LMA), leaf thickness (T_{leaf}), leaf vein density (VLA), and free ending vein number per leaf area (FEV) in seven species

Species	Species symbol	Family	Habit	Drought sensitivity	LMA (g m^{-2})	T_{leaf} (mm)	VLA (mm mm^{-2})	FEV (mm^{-2})
Nerium oleander	No	Apocynaceae	Shrub	Tolerant[1, 2]	151.5 ± 11.7^{a}	1.63 ± 0.02^{a}	12.0 ± 0.9^{c}	2.82 ± 0.70^{c}
Platanus occidentalis	Po	Platanaceae	Tree	Moderately tolerant [3]	99.8 ± 5.5^{c}	0.72 ± 0.03^{c}	11.9 ± 1.1^{c}	7.21 ± 1.05^{ab}
Glycine max	Gm	Fabaceae	Crop/herb	Sensitive [4, 5]	32.7 ± 2.1^{f}	0.91 ± 0.04^{b}	7.8 ± 1.0^{e}	3.50 ± 0.55^{c}
Populus nigra	Pn	Salicaceae	Tree	Moderately tolerant[6]	63.2 ± 4.0^{e}	0.92 ± 0.02^{b}	14.5 ± 0.9^{b}	5.50 ± 0.50^{b}
Ginkgo biloba	Gb	Ginkgoaceae	Tree	Moderately sensitive[7]	96.5 ± 3.6^{c}	0.36 ± 0.01^{d}	1.8 ± 0.1^{g}	-
Ceratonia siliqua	Cs	Fabaceae	Tree	Tolerant[8]	110.2 ± 6.1^{b}	1.55 ± 0.03^{a}	15.7 ± 1.0^{a}	3.70 ± 0.90^{c}
Gossypium hirsutum	Gh	Malvaceae	Crop/shrub	Moderately sensitive[9]	77.7 ± 5.3^{d}	0.71 ± 0.02^{c}	10.4 ± 0.6^{d}	8.80 ± 0.70^{a}

[1]Kumar et al. (2017); [2]Lenzi et al. (2009); [3]Tschaplinski and Norby (1991); [4]Desclaux and Roumet (1996); [5]Li et al. (2013); [6]Viger et al. (2016); [7]Kagotani et al. (2016); [8]Lo Gullo et al. (2003); [9]Ullah et al. (2008)

Data are mean ± SD

Different letters indicate statistical differences (Tukey's HSD test, $p < 0.05$)

deficit (VPD) inside the chamber was 1.73 ± 0.4 kPa. After the leaf reached a steady state (the fluctuation of stomatal conductance g_s being less than 0.05 mol m^{-2} s^{-1} during a 10-min period), the auto-progress of the CO_2 response curve was adopted. The reference CO_2 concentrations were subsequently set at 400, 300, 200, 100, 50, 400, 600, 800, 1000, 1200, 1500, 2000, 400 µmol CO_2 mol^{-1} air. The CO_2 response curve measurements were performed between 8:30 am and 11:30 am each day.

As described in our previous study (Xiong and Flexas 2021), the mesophyll conductance (g_m) was calculated based on Fick's first law of diffusion:

$$g_m = \frac{A}{C_i - C_c}, \tag{1}$$

where the net photosynthetic rate (A), and the intercellular CO_2 concentration (C_i) were taken from the gas exchange measurements. And the chloroplast CO_2 concentration (C_c) was estimated based on the Harley et al. (1992) method:

$$C_c = \frac{\Gamma * \left(J + 8\left(A + R_d\right)\right)}{J - 4\left(A + R_d\right)} \tag{2}$$

The electron transport rate (J) was directly taken from the Li-COR 6400 measurement. The Γ* represents the CO_2 compensation point in the absence of respiration (taken as 40 µmol mol^{-1} in this study), and the R_d represents the day respiration rate, which was fitted from the CO_2 response curve. For each data point generated, we checked whether it met the reliability criterion ($10 > dC_c/dA > 50$), as suggested by Harley et al. (1992).

The relative photosynthetic limitations of stomatal conductance (l_s), mesophyll conductance (l_s), and photosynthetic biochemistry (l_b) were calculated according to Grassi and Magnani (2005).

$$l_s = \frac{g_t/g_s \cdot \partial A/\partial C_c}{g_t + \partial A/\partial C_c} \tag{3}$$

$$l_m = \frac{g_t/g_m \cdot \partial A/\partial C_c}{g_t + \partial A/\partial C_c} \tag{4}$$

$$l_b = \frac{g_t}{g_t + \partial A/\partial C_c}, \tag{5}$$

where the g_t represents the total CO_2 diffusion conductance ($1/g_t = 1/g_s + 1/g_m$).

In addition, the maximum carboxylation rate (V_{cmax}), the maximum electron transport rate (J_{max}), and the g_m independent of chlorophyll fluorescence (g_mE) were fitted from CO_2 response curves (Ethier and Livingston 2004).

Leaf hydraulic vulnerability and pressure–volume curve

K_{leaf} vulnerability curves were measured using the evaporative flux method (Scoffoni et al. 2011). Mature and sun-exposed branches were collected from five to forty-five individuals per species in field conditions, except for *G. max*, and *G. hirsutum*, for which 30 to 40 entire plants (keeping the root system intact as possible) with at least three new fully expanded leaves were collected. Then, the branches or

entire plants were covered with two layers of black plastic bags and rehydrated overnight. Branches were cut into segments with at least three leaves under deionized water and then bench dried to create a range of leaf water potentials for vulnerability curves measurement. Dehydrated branches were placed into a sealable bag for leaf water potential. Samples were allowed to equilibrate for at least 15 min before two leaves were excised and measured for initial water potential ($\psi_{initial}$, the average water potential of two leaves) using a pressure chamber (PMS 1505D, PMS Instrument Co., Albany, OR, USA). If the difference in the leaf water potential of those two leaves was greater than 0.25 MPa, the shoot was discarded. The third leaf (typically the middle one) measured K_{leaf}.

The details about K_{leaf} measurements were described in our previous studies (Xiong et al. 2017, 2018; Wang et al. 2022). In brief, leaves were cut from the branches with a fresh razor blade under ultrapure water. Then the petiole was rapidly connected to silicone tubing underwater to prevent air from entering the system. The tubing system was connected to a plastic Erlenmeyer flask (250 ml) with degassed pure water on an analytical balance (ABT 320-4 M, KERN, Balingen, Germany). The leaks of the tubing system were carefully checked before the measurement was conducted (see details in Xiong et al. 2018). The light intensities (light source: APO4, Eiviled 2010, Illes Balears, Spain) on the leaf surface were 1500 ± 65 µmol m^{-2} s^{-1}, as measured with a quantum sensor (Li-190R, LI-COR, Lincoln, NE, USA). Leaf temperature was controlled between 23 and 27 °C by adjusting the room air temperature using an air conditioner.

The weight of water loss was recorded every 60 s, and the transpiration flux rate was calculated as the slope of the linear regression between weight and time for every 6 minutes. For each leaf, the duration of the steady transpiration was not short than 15 min. After the leaves were removed from the tubing system and kept in darkness (in Ziploc Smart Zip Freezer Bags) to equilibrate for at least 20 min and then, the final leaf water potential (ψ_{final}) was measured with a pressure chamber (Model 1505, PMS Instrument Company, Albany, USA). The leaf areas of the leaves were measured from digitalized pictures using Image J (https://imagej.nih.gov/ij/), and water flux rate (E) of each leaf was normalized by its leaf area K_{leaf} was calculated as follows:

$$K_{leaf} = \frac{E}{\Psi_{water} - \Psi_{final}}. \quad (6)$$

where the Ψ_{water} is the water potential of distilled water (= 0 MPa).

As discussed in several previous studies (Scoffoni et al. 2012; Wang et al. 2018, 2022), dehydrated leaves may recover in leaf water potential before reaching steady-state transpiration during the evaporative flux method (EFM) measuring due to the stomata opening and the ψ_{final} is less negative than $\psi_{initial}$. Alternatively, the transpiration rate may be sufficient for ψ_{final} to be driven lower than $\psi_{initial}$. According to the suggestion of those studies we constructed vulnerability curves by plotting K_{leaf} against whichever was the lowest, ψ_{final} or $\psi_{initial}$ ('ψ_{lowest}'), that is, the leaf water potential associated with the strongest dehydration experienced during the experiment, and each leaf was considered as a data point. In the current study, the maximum leaf hydraulic conductance (K_{max}) of each species was calculated as the average K_{leaf} for the points above − 0.5 MPa of the vulnerability curves. Five pressure–volume curves per species were conducted to estimate osmotic potential at full turgor (π_0; MPa) and at turgor loss point (π_{tlp}; MPa), and modulus of elasticity (ε; MPa) as in Sack and Pasquet-Kok (2011).

Leaf vein density

Leaves were chemically cleared in 15% NaOH (w/v) and then bleached following our previous standard protocol (Xiong et al. 2018), and then stained with safranin and fast green in ethyl alcohol. After washing redundant safranin and fast green in the water, leaves were scanned to measure major vein length, and the minor vein densities were measured from pictures captured using a light microscope (U-TVO.5XC; Olympus, Tokyo, Japan). Leaf area and vein length were manually measured by using ImageJ (more details see our previous studies, Xiong et al. 2018). In this study, the major vein is defined as the sum the 1°, 2° and 3° veins and the veins of any order higher than 3° were considered minor veins. In this case, *G. biloba* only has the major veins (Fig. S1).

Light microscopy analysis

Small leaf discs of about 4.0 × 1.2 mm were also cut from the middle of new fully expanded leaves after the gas exchange measurement. In a vacuum chamber, the leaf discs were infiltrated with fixative 2.5% glutaric aldehyde in 0.1 M phosphate buffer (pH = 7.6) at 4 ℃, and post-fixed in 2% buffered osmium tetroxide at 20 ℃ for two h. The samples were embedded in Spurr's epoxy resin. For light microscopy, semithin leaf cross-sections were cut using a fully automated rotary microtome (Leica RM2265, Leica Microsystems, Milton Keynes, UK). The leaf sections were stained with 1% (w/v) toluidine blue in 1% (w/v) $Na_2B_4O_7$, and they were examined at 40 × and 100 × magnification with an Olympus IX71 light microscope (Olympus Optical, Tokyo, Japan). As for the transmission electron microscope (TEM), H-7650 (Hitachi—Science & Technology, Tokyo, Japan) was used for observation and photography. Three leaves per species were analyzed. The total cross-sectional area of mesophyll tissues (S_{mes}) and intercellular air space area (S_{ias}), the total

length of the mesophyll cell wall exposed to intercellular air space (l_{mes}), the total length of chloroplasts touching the plasma membrane appressed to intercellular air space (l_c), cell wall thickness (T_{cw}), and the width of the analyzed leaf cross-section (L) were measured using Image J software (National Institute of Health, Bethesda, MD, USA). The volume fraction of intercellular air space (f_{ias}) was calculated as follows:

$$f_{ias} = \frac{S_{ias}}{S_{mes}} \tag{7}$$

S_m and S_c were then calculated as follows:

$$S = \frac{l}{L} \times F, \tag{8}$$

where S is S_m or S_c, l is l_{mes} or l_c, and the F is the curvature correction factor, which was measured and calculated for each species according to Tomás et al. (2013) for palisade and spongy cells by measuring their width and height and calculating an average width/height ratio. The curvature factor correction ranged from 1.09 to 1.54 for spongy cells and 1.38 to 1.61 for palisade cells.

Statistical analysis

One-way ANOVA analysis was used to test the differences in measured traits among species. Regression analyses were performed with mean values to test the correlations between parameters, and the PCA analysis was performed using FactoMineR (Lê et al. 2008). To identify the 'best' vulnerability curve for each species, four different mathematical functions fit the Ψ_{lowest} and K_{leaf} data using *orthogonal nonlinear least-squares regression* approach (Wang et al. 2018). Linear $\left(K_{leaf} = a \cdot \Psi_{lowest} + b\right)$, Sigmoidal $\left(K_{leaf} = \frac{a}{1+e^{-\left(\frac{\Psi_{lowest}-c}{b}\right)}}\right)$, exponential $\left(K_{leaf} = \frac{a}{1+\left(\frac{\Psi_{lowest}}{c}\right)^{b}}\right)$, and logistic $\left(K_{leaf} = c + ae^{-b\Psi_{lowest}}\right)$ curves were fitted to these data. The curve with the lowest Akaike Information Criteria (AIC) and/or Bayesian information criterion (BIC) values were selected as the 'best' fit (Table S1). All analyses were performed in R version 3.5.1 (R Core Team 2018).

Results

Traits diversity

Across the 7-species, there were substantial differences in leaf mass per area (LMA), leaf thickness (T_{leaf}), and vein length per area (VLA; Table 2 & Fig.S1). The LMA varied from 32.7 in *G. max* to 151.5 g m^{-2} in *N. oleander*; T_{leaf} from 0.36 in *G. biloba* to 1.63 mm in *N. oleander*; VLA from 1.8 in *G. biloba* to 15.7 mm mm^{-2} in *C. siliqua*; and FEV from 0 in *G. biloba* to 8.8 mm^{-2} in *G. hirsutum*. Across the estimated species, the major and minor vein density also showed large variation. Species varied by 4.4-fold in major vein length and 4.1-fold in minor vein length (Table S2). Like the leaf veins, the mesophyll structures also showed large differences across species (Fig. S1; Table S2). In *P. nigra*, 40.9% of the cross-section was occupied by intercellular air space (f_{IAS}); however, the f_{IAS} in *N. oleander* was only 15.2% (Table S2). There was also a significant variation in the S_m (a minimum of 19.7 m^2 m^{-2} in *N. oleander* and a maximum of 31.1 m^2 m^{-2} in *G. hirsutum*), S_c (a minimum of 10.2 m^2 m^{-2} in *G. biloba* and maximum of 28.8 m^2 m^{-2} in *G. max*) and T_{cw} (a minimum of 0.197 µm in *N. oleander* and maximum of 0.431 µm in *G. biloba*).

Across all selected species, the saturated photosynthetic rate (A) varied from 7.3 µmol m^{-2} s^{-1} in *G. biloba* to 27.6 µmol m^{-2} s^{-1} in *G. hirsutum* (Table 3). Stomatal

Table 3 Mean values for the photosynthetic parameters at 25 ℃

Species	A (µmol m^{-2} s^{-1})	g_s (mol m^{-2} s^{-1})	g_m (mol m^{-2} s^{-1})	g_mE (mol m^{-2} s^{-1})	V_{cmax} (µmol m^{-2} s^{-1})	J_{max} (µmol m^{-2} s^{-1})
Nerium oleander	10.3 ± 0.9 d	0.10 ± 0.05 d	0.13 ± 0.01c	0.14 ± 0.02 c	40.9 ± 7.4 f	78.9 ± 6.7 d
Platanus occidentalis	14.1 ± 0.4 c	0.18 ± 0.02 c	0.14 ± 0.03 c	0.34 ± 0.13 a	68.1 ± 7.0 c	139.6 ± 17.1 b
Glycine max	16.5 ± 0.9 b	0.24 ± 0.01 b	0.22 ± 0.02 b	0.37 ± 0.07 a	67.6 ± 3.5 c	125.5 ± 11.9 b
Populus nigra	15.1 ± 1.9 bc	0.22 ± 0.04 b	0.20 ± 0.05 b	0.18 ± 0.03 b	61.2 ± 7.4 d	121.4 ± 18.8 bc
Ginkgo biloba	7.3 ± 0.1 e	0.08 ± 0.01 e	0.08 ± 0.01d	0.10 ± 0.02 d	36.6 ± 0.4 g	81.5 ± 6.2 d
Ceratonia siliqua	13.6 ± 1.0 c	0.16 ± 0.01 c	0.14 ± 0.02 c	0.11 ± 0.03 cd	54.9 ± 3.6 e	113.3 ± 16.4 c
Gossypium hirsutum	27.6 ± 0.2 a	0.30 ± 0.02 a	0.31 ± 0.03 a	0.38 ± 0.06 a	135.2 ± 5.9 a	233.7 ± 35.3 a

Data are mean ± SD. Different letters indicate statistical differences (Tukey's HSD test, $p < 0.05$)

A light-saturated photosynthetic rate, g_s stomatal conductance, g_m mesophyll conductance, g_mE mesophyll conductance fitted from CO_2 response curve, V_{camx} maximum carboxylation efficiency, J_{max} maximum electron transport rate

conductance to CO_2 (g_s) ranged 3.6-fold, and mesophyll conductance to CO_2 (g_m) ranged 3.7-fold. The largest g_s and g_m were observed in *G. hirsutum*, and the lowest in *G. biloba*. In addition, both the maximum carboxylation rate of rubisco (V_{cmax}) and maximum electron transportation rate (J_{max}) varied greatly among species (Table 3).

Leaf hydraulic vulnerability and pressure–volume curves

The shape of vulnerability curves for K_{leaf} differed substantially across species (Fig. S2, Table S1). Species varied significantly in aspects of leaf hydraulic vulnerability curve and pressure–volume curve parameters (Table 4). The maximum leaf hydraulic conductance (K_{max}) varied from 5.05 to 13.5 mmol m^{-2} s^{-1} MPa^{-1} (Table 4). The P_{50} varied from − 0.72 to − 2.24 MPa in *G. hirsutum* and *N. oleander*, respectively; and in P_{80} from − 1.22 to − 3.97 MPa in the same two species. However, the 0.05 level of confidence intervals for both P_{50} and P_{80} were quite large. There was also a significant variation in the π_0 (the highest being − 1.05 MPa in *G. max* and the lowest − 2.38 MPa in *N. oleander*), π_{tlp} (the highest being − 1.41 MPa in *G. max* and the lowest -3.32 MPa in *N. oleander*) and Ɛ (a minimum of 8.9 MPa in *N. oleander* and maximum of 16.0 MPa in *P. nigra*).

Trait correlations

We first analyzed the correlations among tolerance traits and found that K_{leaf} vulnerability traits (P_{50} and P_{80}) were weakly correlated with pressure volume traits across selected species (Fig. 1). Then, the correlations among efficiency traits were analyzed, and it was found that A was strongly correlated with both g_s ($r^2 = 0.88$; $p = 0.002$; Fig. 2d), g_m ($r^2 = 0.86$; $P = 0.002$; Fig. 2e) and V_{cmax} ($r^2 = 0.96$; $p < 0.001$; Fig. 2f). However, K_{max} was decoupled from gas exchange traits except for g_m ($r^2 = 0.73$; $p = 0.014$; Fig. 2c) across species. Here we also estimated the influences of leaf anatomy on g_m and K_{max}, the results showed that K_{max} was decoupled from VLA, VLA_{major} and VLA_{minor} across species; however, g_m was strongly affected by S_c and T_{cw} (Fig. 3). The correlation analysis between efficiency and tolerance traits showed no correlations between A and P_{50} ($r^2 = 0.2$; $p = 0.315$) or π_{tlp} ($r^2 = 0.31$; $p = 0.199$) across species (Fig. 4). Similarly, no significant correlations were found between K_{max} and P_{50} ($r^2 = 0.06$; $P = 0.61$) as well as π_{tlp} ($r^2 = 0.40$; $p = 0.144$). However, we found that P_{50} positively correlated with VLA_{major} ($r^2 = 0.63$; $p = 0.03$), but not with VLA ($r^2 = 0.074$; $p = 0.554$) and VLA_{minor} ($r^2 = 0.002$; $p = 0.934$) across species (Fig. 5a–c). Moreover, cell wall thickness (T_{cw}) had significant impacts on pressure–volume parameters (Fig. 5d, e, f). The π_0 ($r^2 = 0.84$; $P = 0.004$), π_{tlp} ($r^2 = 0.82$; $P = 0.005$) and ε ($r^2 = 0.62$; $p = 0.037$) significantly correlated with T_{cw}.

The principal component (PCA) analysis results are shown in Fig. 6 and Table S3. The first PCA axis accounted for 52% of the total variation and showed strong loadings on LMA, VLA_{major}, f_{IAS}, gas exchange, leaf hydraulic vulnerability, and pressure–volume traits. The second axis, which accounted for 24.5% of the total variation, had strong loadings on K_{max}, VLA, VLA_{minor} and mesophyll structural traits (Fig. 6a). PCA ordination using all species demonstrated variable combinations of leaf hydraulic, gas exchange traits, leaf anatomy, leaf hydraulic vulnerability, and pressure–volume traits (Fig. 6b).

Discussion

Hydraulic vulnerability traits and pressure–volume traits

Across species, the parameters (P_{50} and P_{80}) of K_{leaf} vulnerability curves were correlated strongly with the parameters

Table 4 Maximum leaf hydraulic conductance (K_{max}), leaf water potential at 50% and 80% decline of leaf hydraulic conductance (P_{50} and P_{80}), osmotic potential at full turgor (π_0) and at turgor loss point (π_{tlp}; MPa), and modulus of elasticity (ε)

Species	K_{max} (mmol m^{-2} s^{-1} MPa^{-1})	P_{50} (− MPa)	P_{80} (− MPa)	π_0 (− MPa)	π_{tlp} (− MPa)	Ɛ (MPa)
Nerium oleander	10.2 ± 1.8^{c}	2.24 (2.14, 2.45)	3.97 (3.86, 4.22)	2.38 ± 0.11^{a}	3.32 ± 0.12^{a}	8.9 ± 0.8^{c}
Platanus occidentalis	7.6 ± 1.2^{d}	1.02 (0.94, 1.32)	1.45 (1.41, 1.49)	1.65 ± 0.05^{c}	2.37 ± 0.18^{c}	15.6 ± 1.1^{a}
Glycine max	11.7 ± 1.6^{b}	1.16 (1.05, 1.28)	1.92 (1.78, 2.04)	1.05 ± 0.05^{e}	1.41 ± 0.18^{f}	11.5 ± 0.8^{b}
Populus nigra	11.6 ± 1.2^{b}	0.87 (0.76, 1.09)	1.26 (0.89, 1.41)	1.17 ± 0.05^{d}	1.55 ± 0.12^{e}	16.0 ± 1.0^{a}
Ginkgo biloba	8.2 ± 0.5^{d}	0.89 (0.41, 1.32)	1.91 (1.35, 2.04)	2.03 ± 0.06^{b}	2.83 ± 0.15^{b}	10.5 ± 1.4^{b}
Ceratonia siliqua	5.05 ± 0.7^{e}	1.41(1.24, 1.84)	2.19 (2.01, 2.36)	2.09 ± 0.18^{ab}	2.91 ± 0.14^{b}	9.9 ± 1.6^{bc}
Gossypium hirsutum	13.5 ± 4.9^{a}	0.72 (0.31, 1.04)	1.22 (0.66, 1.65)	1.39 ± 0.06^{d}	1.97 ± 0.12^{d}	14.9 ± 1.8^{a}

Different letters indicate statistical differences (Tukey's HSD test, $p < 0.05$)

Values are mean ± sd, and for P50 and P80, the 95% confidence intervals were shown in brackets

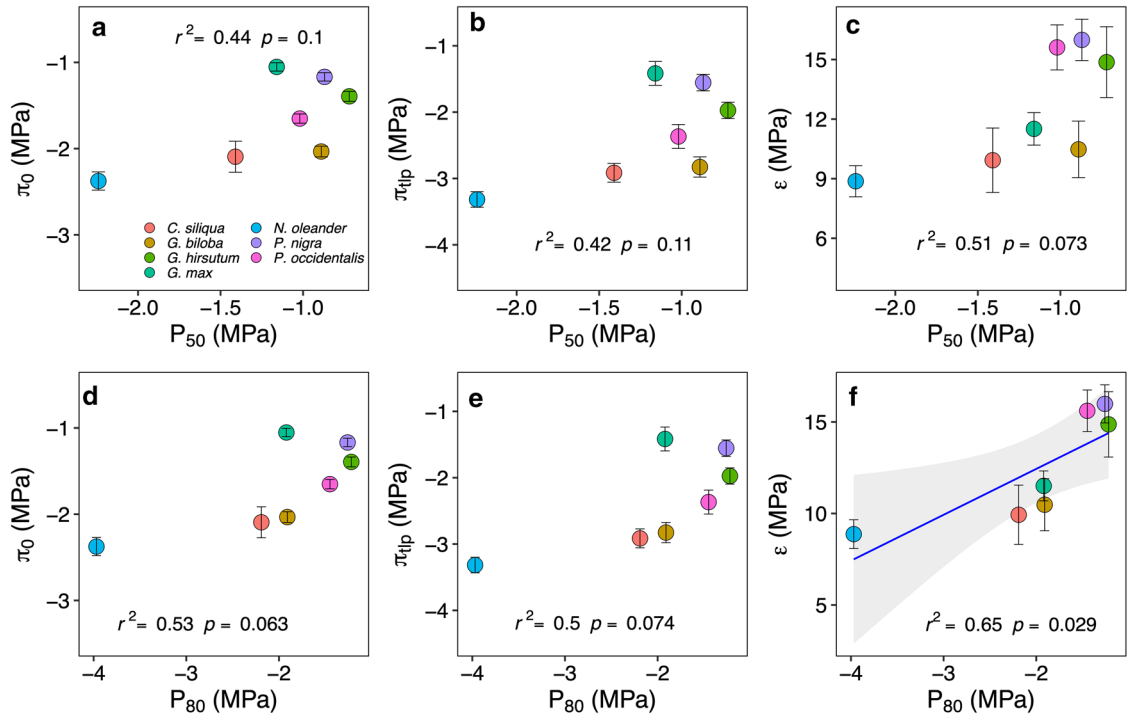

Fig. 1 Correlations among pressure–volume curve traits and leaf hydraulic vulnerability curve traits. Lines were fitted using a linear model, and the shade areas around lines indicate the 95% of confidence intervals. $\pi_{0,}$ osmotic potential at full rehydration; π_{tlp}; turgor loss point; ε, modulus of elasticity; P_{50}, leaf water potential at a 50% of maximum leaf hydraulic conductance lost; and P_{80}, leaf water potential at an 80% of maximum leaf hydraulic conductance lost. The full names for each of the species are provided in Table 2

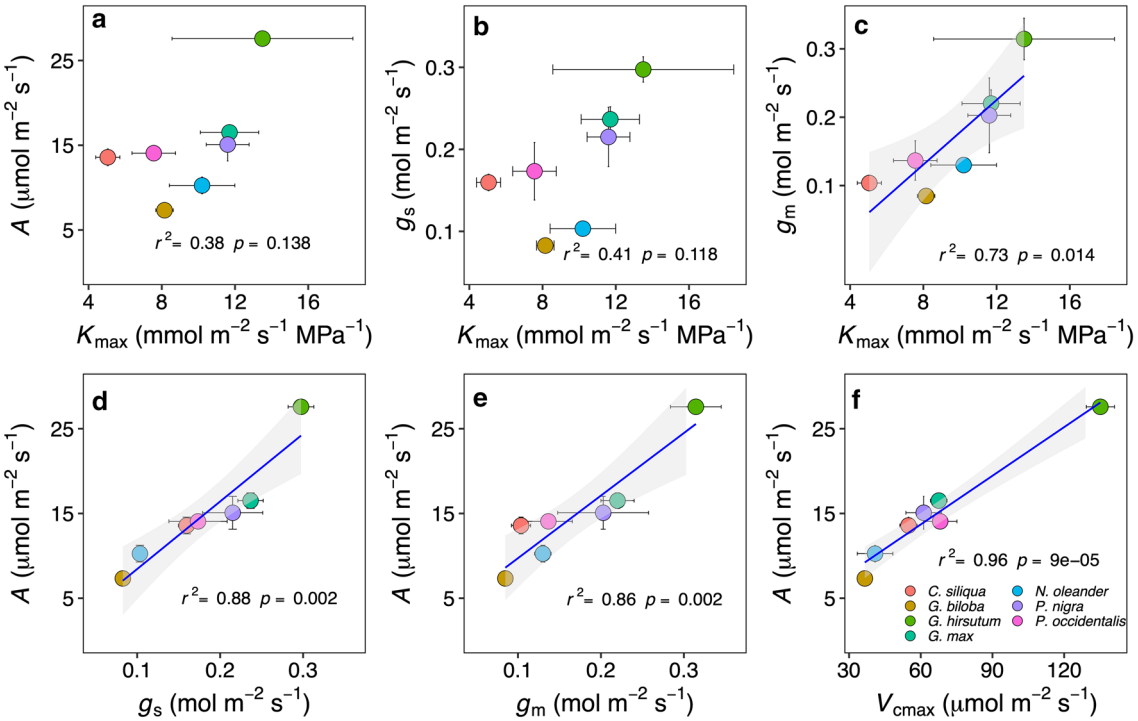

Fig. 2 Correlations among efficiency traits. The correlation between traits was fitted using the linear model, and the shade areas around lines indicate the 95% of confidence intervals. *A*, light-saturated photosynthetic rate; K_{max}, maximum leaf hydraulic conductance; g_s, stomatal conductance; g_m, mesophyll conductance; and V_{camx}, maximum carboxylation efficiency

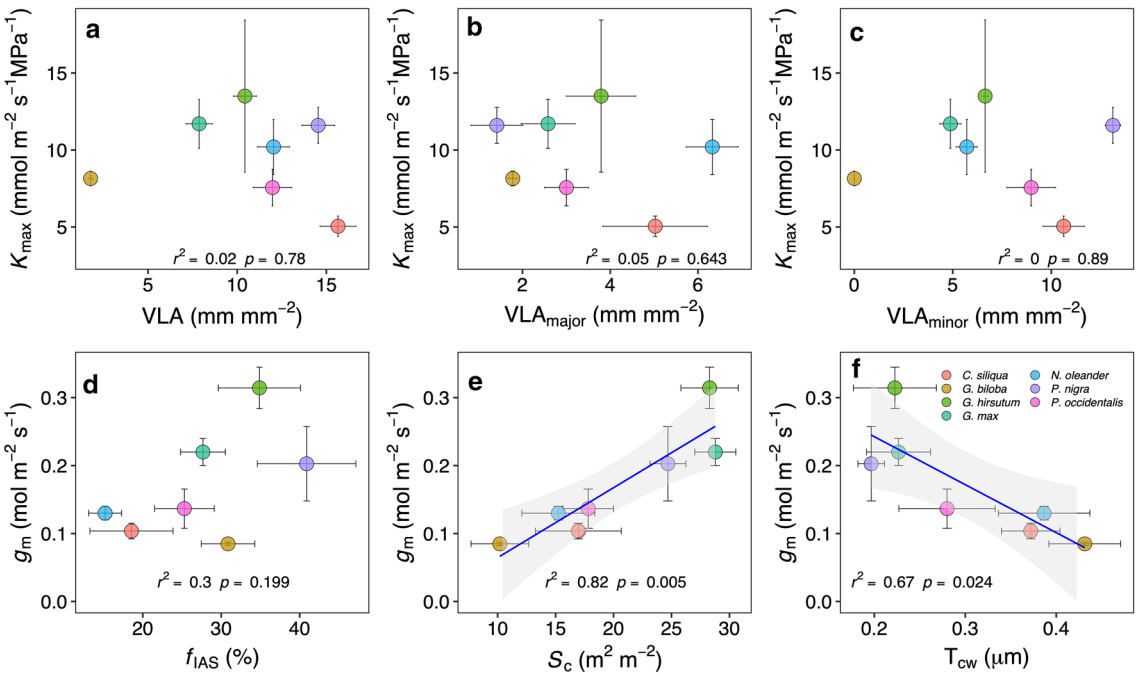

Fig. 3 Impacts of leaf anatomical traits on mesophyll conductance (g_m) and maximum leaf hydraulic conductance (K_{max}). VLA. Leaf vein density; VLA$_{major}$, major vein density; VLA$_{minor}$, minor vein density; f_{IAS}, fraction of leaf mesophyll volume occupied by intercellular air space; S$_c$, total chloroplast surface area exposed to intercellular air space per unit of leaf surface area; and T$_{cw}$, cell wall thickness

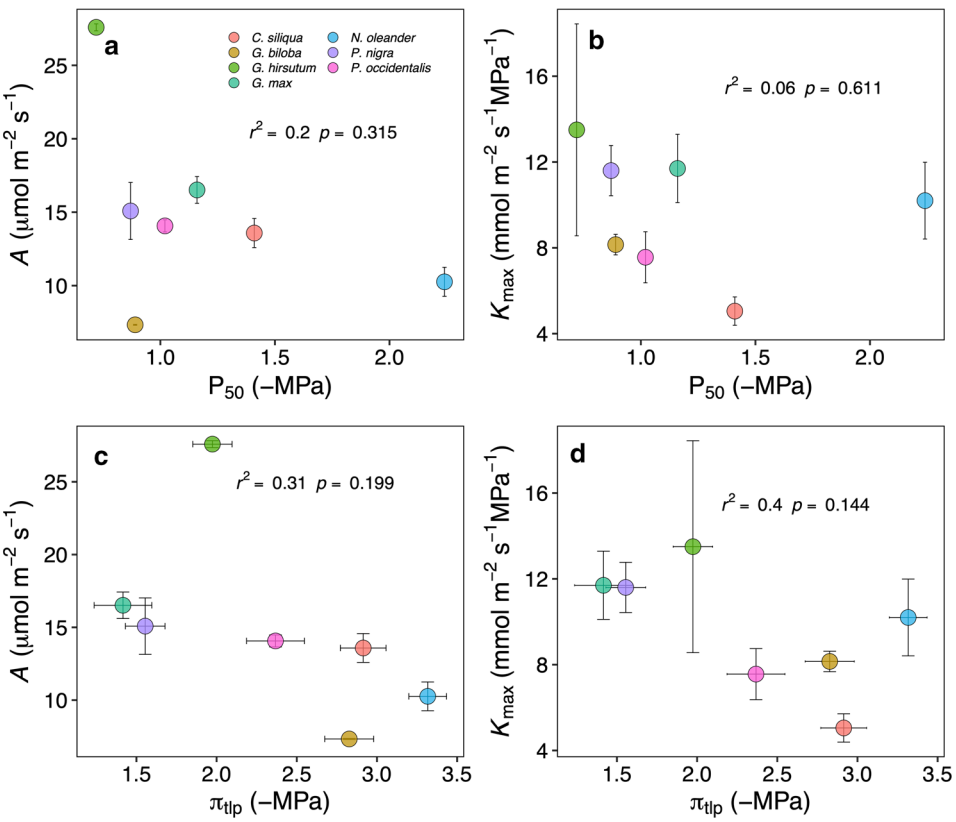

Fig. 4 Efficiency vs safety across species. **a**, **b** Correlations of leaf water potential at a 50% of maximum leaf hydraulic conductance lost (P$_{50}$) to light-saturated photosynthetic rate (A) and maximum leaf hydraulic conductance (K_{max}); and **c**, **d** correlations of osmotic potential at the turgor point loss point (π_{tlp}) to A and K_{max}

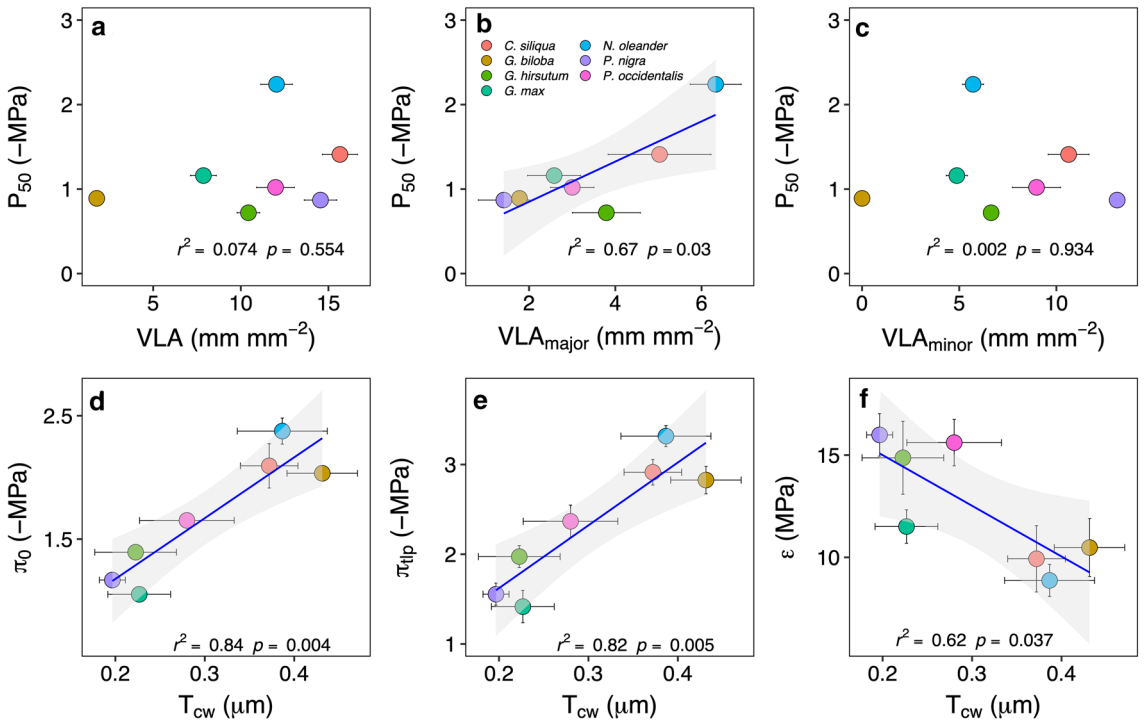

Fig. 5 Influences of leaf **a** vein density (VLA), **b** major vein density (VLA_{major}), and **c** minor vein density (VLA_{minor}) on the leaf water potential at a 50% of maximum leaf hydraulic conductance lost (P_{50}); and the influences of cell wall thickness (T_{cw}) on **d** osmotic potential at full rehydration (π_0); **e** turgor loss point (π_{tlp}) and **f** modulus of elasticity (ε)

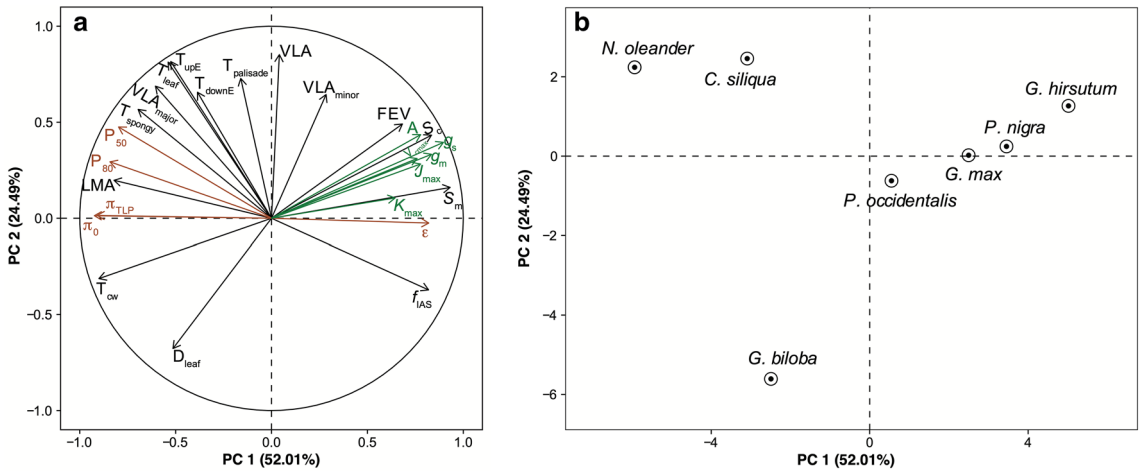

Fig. 6 Principal component analysis (PCA) of gas exchange, leaf hydraulic, hydraulic vulnerability, press-volume, and leaf anatomical traits. The symbols used for each trait represented in the axis titles are provided in Table 1 and the full names for each of the species are provided in Table 2

(π_0, π_{tlp}, ε) of pressure–volume curves, as observed in previous studies (Blackman et al. 2010; Scoffoni et al. 2012; Powell et al. 2017; Figs. 1, 6a; Fig. S6). Our results together with earlier studies suggest that K_{leaf} vulnerability traits and pressure–volume traits are co-selected in species with large drought tolerance. The embolization of the xylem conduits has been widely believed to be the major cause of hydraulic decline during drought, and K_{leaf} vulnerability curve was widely used in evaluating the capacity of leaves to avoid xylem embolism in the past (reviewed by Scoffoni et al., 2012). The tight correlations between K_{leaf} vulnerability traits and pressure–volume traits were hypothesized to arise because cells maintaining turgor at more negative water potentials could preserve cell integrity and, therefore, confer

resistance to K_{leaf} decline (Blackman et al. 2010; Scoffoni et al. 2016a). However, several recent studies highlighted that the decline of K_{leaf} during dehydration is caused by the decrease of outside xylem hydraulic conductance (K_{ox}) rather than the hydraulic conductance inside xylem (K_x) (Trifiló et al. 2016; Scoffoni et al. 2017). If this were the case, then the K_{leaf} vulnerability parameters would mainly reflect the drought tolerance of mesophyll tissues as pressure–volume parameters do. Unfortunately, we cannot test this question as we did not separate the contributions of K_x and K_{ox} on K_{leaf} vulnerability in this study.

Hydraulic conductance and gas exchange efficiency

Although K_{max} and gas exchange traits varied greatly among species with different growth habits, no significant correlations between K_{max} and gas exchange traits except g_m were observed in the current study (Fig. 2). This result consisted with a previous one on nine C_4 grasses (Ocheltree et al. 2016); however, it was opposite to other studies which observed strong correlations between K_{max} and gas exchange traits explained as coordinated evolution of these processes (Brodribb et al. 2007; Scoffoni et al. 2016b). Lacking a correlation between K_{max} and A in the present study unlikely results from the smaller set of species because the variability in both A and K_{max} among our species was similar to that in the previous studies (Brodribb et al. 2007; Ocheltree et al. 2016; Scoffoni et al. 2016b).

The coordination theory of K_{leaf} and gas exchange is based on the following two assumptions: (i) leaf is the bottleneck of plant hydraulics system, and (ii) stomatal resistance is the major limiting factor to A (Brodribb et al. 2007; Scoffoni et al. 2016b). During photosynthesis, the ability to keep the stomata opening to capture CO_2 depends on the plant's capacity to replace that water lost through stomata. Hence, the whole plant hydraulic conductance should match g_s to maximize photosynthesis. By performing a literature synthesis analysis, Sack and Holbrook (2006) summarized that leaves contributed on average to about 30% of whole plant hydraulic resistance and suggested that leaf is the bottleneck of plant hydraulic system, although with large variations across species and environmental conditions (Sack and Holbrook 2006). Conversely, many direct investigations suggested that the root is the major bottleneck in the plant hydraulics (Steudle 2000; Domec et al. 2009), also varying greatly across species and growth conditions. For instance, due to the existence of strong aerenchyma and apoplastic barriers in roots, the radial, as well as the axial water transport capacities in roots, were strongly limited in wet habit species (Steudle 2000; Ranathunge et al. 2005; Kotula et al. 2009). Therefore, the variable contributions of leaves and roots to plant hydraulic resistance between species may be one of the reasons for the decoupled correlation between K_{max} and gas exchange traits. Further studies are needed to check the contributions of roots and leaves on plants hydraulic systems across species with variable growth conditions. In the current study, a tight correlation between A and g_s indicated that g_s could be one of the major photosynthetic limiting factors. However, the limitation analysis showed that the relative contributions of g_s, g_m, and biochemistry factors to A varied widely across species, and the A of the selected species was largely constricted by biochemical factors despite g_s and g_m contributing nearly half of the limitation to A in some of species (Fig. S3). While in gymnosperms (represented here by *Ginkgo*), despite g_s and g_m are generally far larger photosynthetic limitations than biochemistry, and in angiosperms, all three limitations are similar on average (Gago et al. 2019), biochemical limitations tend to be larger in crops (Nadal and Flexas 2018, 2019). In the present study, we include two true crops, cotton and soybean) plus four fast-growing woody species often used as crops (*Populus*, *Ceratonia*, *Nerium,* and *Platanus*), which could be the predominance of biochemical limitations in this survey. In fact, the other species (*Ginkgo*) present the lowest biochemical limitations among the seven studied species. Regardless of the reason, the reality is that in the species selected, the stomatal limitation is not the largest limitation to photosynthesis, being thus another possible explanation for the coordination between K_{leaf} and gas exchange.

Safety vs efficiency tradeoff

In the current study, we investigated the leaf level safety and efficiency tradeoffs by measuring leaf hydraulic vulnerabilities, pressure–volume curves, carbon assimilation efficiency and water transport efficiency. No significant tradeoffs between hydraulic safety and efficiency traits on leaf level were observed in our study (Fig. 4), and this result contrasts with several previous studies (Nardini et al. 2012; Ocheltree et al. 2016). Some species seem to have low carbon assimilation efficiency and low drought tolerance, which cannot be considered a strict tradeoff. However, it is true that we did not find any species with large efficiency and large tolerance, for which some tradeoff-like mechanisms may still operate at that level. Furthermore, the principal component analysis confirmed that efficiency traits were largely independent of safety traits (Fig. 6). Further analysis showed that carbon assimilation efficiency traits (gas exchange trait) are related to S_m, S_c, FVE, and VLA_{minor}, while drought tolerance traits are more related to VLA_{major}, T_{cw}, LMA, and thickness of up and low epidermis (Fig. 6); the lack of tradeoffs between efficiency and tolerance traits across species may be thus explained by different leaf anatomical features setting ones and others.

The correlation between K_{leaf} and VLA was often estimated in previous studies, and a higher VLA is predicted

to have both higher K_x and K_{ox}: the former by providing more parallel flow paths through the vein system, and the latter by decreasing horizontal path length for water transport from the veins to the sites of evaporation (Brodribb et al. 2007; Buckley et al. 2015). In the current study, K_{max} was independent of VLA, $VLA_{major,}$ and VLA_{minor}, which was in contrast with some of previous studies (Sack and Frole 2006; Brodribb et al. 2007), but consistent with others (Nardini et al. 2014; Caringella et al. 2015; Xiong et al. 2015). In fact, beyond VLA, K_{leaf} is also influenced by many other anatomical traits, such as leaf thickness, mesophyll tissue thickness, the size of bundle sheath cells and bundle sheath extensions, and biochemistry traits, including aquaporins mediated membrane permeability (Sade et al. 2014; Secchi and Zwieniecki 2014; Buckley et al. 2015; Caringella et al. 2015). However, we did not estimate the bundle sheath and bundle sheath extension traits nor biochemical traits. Further research is needed to uncover the role of leaf vein traits in determining K_{leaf} by choosing a plant set with a background of other similar traits. Leaf vein traits have also been suggested to influence leaf hydraulic vulnerability. Leaf dehydration may lead to embolism in the vein xylem, leading to a decline of K_x and thus to a decline K_{leaf}. In the present study, we found that P_{50} tightly correlated with VLA_{major} (Fig. 3), which agrees with cavitation events shown to occur in leaf petioles or midribs using a range of hydraulic measurements and visualization approaches (Blackman et al. 2010; Brodribb et al. 2016; Scoffoni et al. 2016a).

The investigation of the influences of mesophyll anatomical traits on photosynthetic, hydraulic, and pressure–volume traits revealed that mesophyll traits strongly influence g_m and pressure–volume traits; however, the K_{max} is independent of mesophyll traits. Indeed, the strong influences of S_c and T_{cw} on g_m observed here have been reported by many previous studies (Evans et al. 2009; Tomás et al. 2013; Tosens et al. 2016; Xiong et al. 2017), and our results further demonstrate that the higher g_m in two crops may relate to their low T_{cw} and high S_c. Recently, the question of how mesophyll structural traits influence water transport inside leaves has been discussed (Buckley et al. 2015; Xiong et al. 2017). Our results showed no clear correlations between mesophyll anatomical traits and K_{max}. Indeed, the water transport pathways in mesophyll tissues are complex, and many other traits, including the permeability of membranes and vein features, might play a role in K_{max}. Pressure–volume traits were significantly affected by mesophyll cell wall thickness, for instance, both π_0 and π_{tlp} were positively correlated with T_{cw}, and ε negatively correlated with T_{cw}. Our results support that the cell wall plays an important role in drought tolerance and photosynthesis, which was also highlighted in recent studies (Nadal et al. 2018; Roig-Oliver et al. 2020). However, in the present, we could not find the negative correlation between A and ε described by Nadal et al. (2018), likely because in our species set, A scaled negatively with T_{cw}, as often observed, but ε also scaled negatively with T_{cw} (Fig. 5f). The latter observation is novel and implies that species with thicker cell walls may have instead more elastic tissues (and probably cell walls). This may reflect that while cell walls are important for both drought tolerance and photosynthesis, the cell wall components conferring one or another may differ, as recently shown by Roig-Oliver et al. (2020).

In summary, we have shown that no strict trade-off exists between carbon assimilation efficiency and drought tolerance at the leaf level across species differing in phylogeny, origin, life form, and drought tolerance. Several relationships previously shown in woody angiosperms were not consistent across woody, herb, and crop species in this study. For instance, the K_{max} was decoupled from photosynthetic rate, $P_{50,}$ and leaf vein density. Further analysis indicated that different leaf anatomical traits in determining efficiency and tolerance traits might explain the observed lack of tradeoffs on leaf scale.

Supplementary Information The online version contains supplementary material available at https://doi.org/10.1007/s00442-022-05250-4.

Acknowledgements We thank Dr. Meisha-Marika Holloway-Phillps, Dr. Tom Buckley, Dr. Christine Scoffoni and Prof. Lawren Sack for helpful insights in interpreting K_{leaf} vulnerability curves data; and Dr. Cyril Douthe for his critical comments on the study design.

Author contribution statement DX and JF: conceived and designed the experiments. DX: performed the experiments. DX and JF: analyzed the data. DX: wrote the manuscript; JF: provided editorial advice.

Funding DX was funded by the National Natural Science Foundation of China (No. 32022060). JF was funded by project PGC2018-093824-B-C41 from the Ministerio de Ciencia, Innovación y Universidades and the ERDF (FEDER).

Data availability All relevant data supporting the results presented in this work are available within the article and the supporting materials.

Declarations

Conflict of interest The authors declare that they have no conflicts of interest associated with this work.

References

Bartlett MK, Scoffoni C, Sack L (2012) The determinants of leaf turgor loss point and prediction of drought tolerance of species and biomes. a global meta-analysis. Ecol Lett 15:393–405

Binks O, Meir P, Rowland L, da Costa AC, Vasconcelos SS, de Oliveira AA, Ferreira L, Christoffersen B, Nardini A, Mencuccini M (2016) Plasticity in leaf-level water relations of tropical rainforest trees in response to experimental drought. New Phytol 211:477–488

Blackman CJ, Brodribb T, Jordan GJ (2010) Leaf hydraulic vulnerability is related to conduit dimensions and drought resistance across a diverse range of woody angiosperms. New Phytol 188:1113–1123

Blonder B, Buzzard V, Simova I, Sloat L, Boyle B, Lipson R, Aguilar-Beaucage B, Andrade A, Barber B, Barnes C, Bushey D, Cartagena P, Chaney M, Contreras K, Cox M, Cueto M, Curtis C, Fisher M, Furst L, Gallegos J, Hall R, Hauschild A, Jerez A, Jones N, Klucas A, Kono A, Lamb M, Matthai JD, McIntyre C, McKenna J, Mosier N, Navabi M, Ochoa A, Pace L, Plassmann R, Richter R, Russakoff B, Aubyn HS, Stagg R, Sterner M, Stewart E, Thompson TT, Thornton J, Trujillo PJ, Volpe TJ, Enquist BJ (2012) The leaf-area shrinkage effect can bias paleoclimate and ecology research. Am J Bot 99:1756–1763

Brodribb T, Feild TS, Jordan GJ (2007) Leaf maximum photosynthetic rate and venation are linked by hydraulics. Plant Physiol 144:1890–1898

Brodribb T, Bienaimé D, Marmottant P (2016) Revealing catastrophic failure of leaf networks under stress. Proc Natl Acad Sci USA 113:4865–4869

Buckley TN (2015) The contributions of apoplastic, symplastic and gas phase pathways for water transport outside the bundle sheath in leaves. Plant Cell Environ 38:7–22

Buckley TN, John GP, Scoffoni C, Sack L (2015) How does leaf anatomy influence water transport outside the xylem? Plant Physiol 168:1616–1635

Buckley TN, John GP, Scoffoni C, Sack L (2017) The sites of evaporation within leaves. Plant Physiol 173:1763–1782

Caringella MA, Bongers FJ, Sack L (2015) Leaf hydraulic conductance varies with vein anatomy across *Arabidopsis thaliana* wild-type and leaf vein mutants. Plant, Cell Environ 38:2735–2746

Desclaux D, Roumet P (1996) Impact of drought stress on the phenology of two soybean (*Glycine max* L. Merr) cultivars. Field Crop Res 46:61–70

Domec JC, Noormets A, King JS, Sun GE, McNulty SG, Gavazzi MJ, Boggs JL, Treasure EA (2009) Decoupling the influence of leaf and root hydraulic conductances on stomatal conductance and its sensitivity to vapour pressure deficit as soil dries in a drained loblolly pine plantation. Plant Cell Environ 32:980–991

Ethier GJ, Livingston NJ (2004) On the need to incorporate sensitivity to CO_2 transfer conductance into the Farquhar-von Caemmerer-Berry leaf photosynthesis model. Plant, Cell Environ 27:137–153

Evans JR, Kaldenhoff R, Genty B, Terashima I (2009) Resistances along the CO_2 diffusion pathway inside leaves. J Exp Bot 60:2235–2248

Farrell C, Szota C, Arndt SK (2017) Does the turgor loss point characterize drought response in dryland plants? Plant, Cell Environ 40:1500–1511

Gago J, Carriquí M, Nadal M, Clemente-Moreno MJ, Coopman RE, Fernie AR, Flexas J (2019) Photosynthesis optimized across land plant phylogeny. Trends Plant Sci 24:947–958

Gleason SM, Westoby M, Jansen S, Choat B, Hacke UG, Pratt RB, Bhaskar R, Brodribb T, Bucci SJ, Cao KF, Cochard H, Delzon S, Domec JC, Fan ZX, Feild TS, Jacobsen AL, Johnson DM, Lens F, Maherali H, Martinez-Vilalta J, Mayr S, McCulloh KA, Mencuccini M, Mitchell PJ, Morris H, Nardini A, Pittermann J, Plavcova L, Schreiber SG, Sperry JS, Wright IJ, Zanne AE (2016) Weak tradeoff between xylem safety and xylem-specific hydraulic efficiency across the world's woody plant species. New Phytol 209:123–136

Grassi G, Magnani F (2005) Stomatal, mesophyll conductance and biochemical limitations to photosynthesis as affected by drought and leaf ontogeny in ash and oak trees. Plant Cell Environ 28:834–849

Harley PC, Loreto F, Di Marco G, Sharkey TD (1992) Theoretical considerations when estimating the mesophyll conductance to CO_2 flux by analysis of the response of photosynthesis to CO_2. Plant Physiol 98:1429–1436

Kagotani Y, Nishida K, Kiyomizu T, Sasaki K, Kume A, Hanba YT (2016) Photosynthetic responses to soil water stress in summer in two Japanese urban landscape tree species (*Ginkgo biloba* and *Prunus yedoensis*): effects of pruning mulch and irrigation management. Trees 30:697–708

Kotula L, Ranathunge K, Steudle E (2009) Apoplastic barriers effectively block oxygen permeability across outer cell layers of rice roots under deoxygenated conditions. roles of apoplastic pores and of respiration. New Phytol 184:909–917

Kumar D, Hassan MA, Miguel AN, Veena A, Monica B, Oscar V (2017) Effects of salinity and drought on growth, ionic relations, compatible solutes and activation of antioxidant systems in oleander (*Nerium oleander* L.). PLoS ONE 12:e0185017

Lê S, Josse J, Husson F (2008) FactoMineR : an R package for multivariate analysis. J Stat Soft 25:18

Lenzi A, Pittas L, Martinelli T, Lombardi P, Tesi R (2009) Response to water stress of some oleander cultivars suitable for pot plant production. Sci Hortic 122:426–431

Li D, Liu H, Qiao Y, Wang Y, Cai Z, Dong B, Shi C, Liu Y, Li X, Liu M (2013) Effects of elevated CO_2 on the growth, seed yield, and water use efficiency of soybean (*Glycine max* (L.) Merr.) under drought stress. Agric Water Manag 129:105–112

Liu H, Ye Q, Gleason SM, He P, Yin D (2021) Weak tradeoff between xylem hydraulic efficiency and safety: climatic seasonality matters. New Phytol 229:1440–1452

Lo Gullo MA, Nardini A, Trifilò P, Salleo S (2003) Changes in leaf hydraulics and stomatal conductance following drought stress and irrigation in *Ceratonia siliqua* (Carob tree). Physiol Plant 117:186–194

Nadal M, Flexas J (2018) Chapter 17 - Mesophyll conductance to CO_2 diffusion: Effects of drought and opportunities for improvement. In: García-Tejero IF, Zuazo VH (eds) Water scarcity and sustainable agriculture in semiarid environment. Academic Press, Amsterdam, pp 403–438

Nadal M, Flexas J (2019) Variation in photosynthetic characteristics with growth form in a water-limited scenario: implications for assimilation rates and water use efficiency in crops. Agric Water Manag 216:457–472

Nadal M, Flexas J, Gulías J (2018) Possible link between photosynthesis and leaf modulus of elasticity among vascular plants. a new player in leaf traits relationships? Ecol Lett 21:1372–1379

Nardini A, Pedà G, La Rocca N (2012) Trade-offs between leaf hydraulic capacity and drought vulnerability: morpho-anatomical bases, carbon costs and ecological consequences. morpho-anatomical bases, carbon costs and ecological consequences. New Phytol 196:788–798

Nardini A, Qunapuu-Pikas E, Savi T (2014) When smaller is better. leaf hydraulic conductance and drought vulnerability correlate to leaf size and venation density across four *Coffea arabica* genotypes. Funct Plant Biol 41:972–982

Niinemets Ü, Portsmuth A, Truus L (2002) Leaf structural and photosynthetic characteristics, and biomass allocation to foliage in relation to foliar nitrogen content and tree size in three *Betula* species. Ann Bot 89:191–204

Ocheltree TW, Nippert JB, Prasad PV (2016) A safety vs efficiency trade-off identified in the hydraulic pathway of grass leaves is decoupled from photosynthesis, stomatal conductance and precipitation. New Phytol 210:97–107

Onoda Y, Wright IJ, Evans JR, Hikosaka K, Kitajima K, Niinemets Ü, Poorter H, Tosens T, Westoby M (2017) Physiological and structural tradeoffs underlying the leaf economics spectrum. New Phytol 214:1447–1463

Powell TL, Wheeler JK, de Oliveira AA, da Costa AC, Saleska SR, Meir P, Moorcroft PR (2017) Differences in xylem and leaf hydraulic traits explain differences in drought tolerance among mature Amazon rainforest trees. Glob Change Biol 23:4280–4293

R Core Team (2018) R: a language and environment for statistical computing. R Foundation for Statistical Computing, Vienna, Austria. https://www.R-project.org/

Ranathunge K, Steudle E, Lafitte R (2005) Blockage of apoplastic bypass-flow of water in rice roots by insoluble salt precipitates analogous to a Pfeffer cell. Plant Cell Environ 28:121–133

Rockwell FE, Holbrook NM, Stroock AD (2014) The competition between liquid and vapor transport in transpiring leaves. Plant Physiol 164:1741–1758

Roig-Oliver M, Nadal M, Clemente-Moreno MJ, Bota J, Flexas J (2020) Cell wall components regulate photosynthesis and leaf water relations of Vitis vinifera cv. Grenache acclimated to contrasting environmental conditions. J Plant Physiol 244:153084

Sack L, Frole K (2006) Leaf structural diversity is related to hydraulic capacity in tropical rain forest trees. Ecology 87:483–491

Sack L, Holbrook NM (2006) Leaf hydraulics. Annu Rev Plant Biol 57:361–381

Sack L, Pasquet-Kok J (2011) Leaf pressure-volume curve parameters. PrometheusWiki /tiki-pagehistory.php?page=Leaf pressure-volume curve parameters&preview=16:(Accessed March 29, 2020).

Sack L, Cowan PD, Jaikumar N, Holbrook NM (2003) The 'hydrology' of leaves. co-ordination of structure and function in temperate woody species. Plant, Cell Environ 26:1343–1356

Sade N, Shatil-Cohen A, Attia Z, Maurel C, Boursiac Y, Kelly G, Granot D, Yaaran A, Lerner S, Moshelion M (2014) The role of plasma membrane aquaporins in regulating the bundle sheath-mesophyll continuum and leaf hydraulics. Plant Physiol 166:1609–1620

Scoffoni C, Rawls M, McKown AD, Cochard H, Sack L (2011) Decline of leaf hydraulic conductance with dehydration. relationship to leaf size and venation architecture. Plant Physiol 156:832–843

Scoffoni C, McKown AD, Rawls M, Sack L (2012) Dynamics of leaf hydraulic conductance with water status. quantification and analysis of species differences under steady state. J Exp Bot 63:643–658

Scoffoni C, Vuong C, Diep S, Cochard H, Sack L (2014) Leaf shrinkage with dehydration: coordination with hydraulic vulnerability and drought tolerance. coordination with hydraulic vulnerability and drought tolerance. Plant Physiol 164:1772–1788

Scoffoni C, Albuquerque C, Brodersen CR, Townes SV, John GP, Cochard H, Buckley TN, McElrone AJ, Sack L (2016a) Leaf vein xylem conduit diameter influences susceptibility to embolism and hydraulic decline. New Phytol 213:1076–1092

Scoffoni C, Chatelet DS, Pasquet-Kok J, Rawls M, Donoghue MJ, Edwards EJ, Sack L (2016b) Hydraulic basis for the evolution of photosynthetic productivity. Nature Plants 2:16072

Scoffoni C, Albuquerque C, Brodersen CR, Townes SV, John GP, Bartlett MK, Buckley TN, McElrone AJ, Sack L (2017) Outside-xylem vulnerability, not xylem embolism, controls leaf hydraulic decline during dehydration. Plant Physiol 173:1197–1210

Secchi F, Zwieniecki MA (2014) Down-regulation of plasma intrinsic protein1 aquaporin in poplar trees is detrimental to recovery from embolism. Plant Physiol 164:1789–1799

Sorek Y, Greenstein S, Netzer Y, Shtein I, Jansen S, Hochberg U (2021) An increase in xylem embolism resistance of grapevine leaves during the growing season is coordinated with stomatal regulation, turgor loss point and intervessel pit membranes. New Phytol 229:1955–1969

Steudle E (2000) Water uptake by roots. Effects of water deficit. J Exp Bot 51:1531–1542

Tomás M, Flexas J, Copolovici L, Galmes J, Hallik L, Medrano H, Ribas-Carbo M, Tosens T, Vislap V, Niinemets Ü (2013) Importance of leaf anatomy in determining mesophyll diffusion conductance to CO_2 across species: quantitative limitations and scaling up by models. quantitative limitations and scaling up by models. J Exp Bot 64:2269–2281

Tosens T, Nishida K, Gago J, Coopman RE, Cabrera HM, Carriquí M, Laanisto L, Morales L, Nadal M, Rojas R, Talts E, Tomás M, Hanba Y, Niinemets Ü, Flexas J (2016) The photosynthetic capacity in 35 ferns and fern allies: mesophyll CO_2 diffusion as a key trait. New Phytol 209:1576–1590

Trifiló P, Raimondo F, Savi T, Lo Gullo MA, Nardini A (2016) The contribution of vascular and extra-vascular water pathways to drought-induced decline of leaf hydraulic conductance. J Exp Bot 67:5029–5039

Trueba S, Pan R, Scoffoni C, John GP, Davis SD, Sack L (2019) Thresholds for leaf damage due to dehydration: declines of hydraulic function, stomatal conductance and cellular integrity precede those for photochemistry. New Phytol 223:134–149

Tschaplinski TJ, Norby RJ (1991) Physiological indicators of nitrogen response in a short rotation sycamore plantation. I. CO_2 assimilation, photosynthetic pigments and soluble carbohydrates. Physiol Plant 82:117–126

Tyree MT, Jarvis PG (1982) Water in tissues and cells. In: Lange OL, Nobel PS, Osmond CB, Ziegler H (eds) Physiological plant ecology II water relations and carbon assimilation. Springer, Berlin Heidelberg, pp 35–77

Ullah I, Rahman M, Ashraf M, Zafar Y (2008) Genotypic variation for drought tolerance in cotton (*Gossypium hirsutum* L.): leaf gas exchange and productivity. Flora 203:105–115

Viger M, Smith HK, Cohen D, Dewoody J, Trewin H, Steenackers M, Bastien C, Taylor G (2016) Adaptive mechanisms and genomic plasticity for drought tolerance identified in European black poplar (*Populus nigra* L.). Tree Physiol 36:909–928

Wang X, Du T, Huang J, Peng S, Xiong D (2018) Leaf hydraulic vulnerability triggers the decline in stomatal and mesophyll conductance during drought in rice (*Oryza sativa*). J Exp Bot 69:4033–4045

Wang X, Zhao J, Huang J, Peng S, Xiong D (2022) Evaporative flux method of leaf hydraulic conductance estimation: sources of uncertainty and reporting format recommendation. Plant Methods 18:63

Wright IJ, Reich PB, Westoby M, Ackerly DD, Baruch Z, Bongers F, Cavender-Bares J, Chapin T, Cornelissen JH, Diemer M, Flexas J, Garnier E, Groom PK, Gulías J, Hikosaka K, Lamont BB, Lee T, Lee W, Lusk C, Midgley JJ, Navas ML, Niinemets Ü, Oleksyn J, Osada N, Poorter H, Poot P, Prior L, Pyankov VI, Roumet C, Thomas SC, Tjoelker MG, Veneklaas EJ, Villar R (2004) The worldwide leaf economics spectrum. Nature 428:821–827

Xiong D, Flexas J (2018) Leaf economics spectrum in rice: leaf anatomical, biochemical and physiological trait trade-offs. J Exp Bot 69:5599–5609

Xiong D, Flexas J (2021) Leaf anatomical characteristics are less important than leaf biochemical properties in determining photosynthesis responses to nitrogen top-dressing. J Exp Bot 72:5709–5720

Xiong D, Yu T, Zhang T, Li Y, Peng S, Huang J (2015) Leaf hydraulic conductance is coordinated with leaf morpho-anatomical traits and nitrogen status in the genus Oryza. J Exp Bot 66:741–748

Xiong D, Flexas J, Yu T, Peng S, Huang J (2017) Leaf anatomy mediates coordination of leaf hydraulic conductance and mesophyll conductance to CO_2 in *Oryza*. New Phytol 213:572–583

Xiong D, Douthe C, Flexas J (2018) Differential coordination of stomatal conductance, mesophyll conductance, and leaf hydraulic conductance in response to changing light across species. Plant, Cell Environ 41:436–450